

## Creating steep density profile with a separatrix

Shun Ogawa<sup>1,2</sup> \* Xavier Leoncini<sup>1</sup> † Alexei Vasiliev<sup>3</sup> ‡ and Xavier Garbet<sup>2</sup> §

1. *Aix Marseille Univ., Univ. Toulon, CNRS, CPT, Marseille, France*

2. *CEA, IRFM, F-13108 St. Paul-lez-Durance cedex, France*

3. *Space Research Institute, Profsoyuznaya 84/32, Moscow 117997, Russia*

The mesoscopic properties of a plasma in a cylindrical magnetic field are investigated from the view point of test-particle dynamics. When the system has enough time and spatial symmetries, a Hamiltonian of a test particle is completely integrable and can be reduced to a single degree of freedom Hamiltonian for each initial state. The reduced Hamiltonian sometimes has an unstable fixed point (saddle point) and a separatrix. Using a maximum entropy principle we compute dynamically compatible equilibrium states of the one particle density function of these systems and discuss how the unstable fixed points affect the density profile or a local pressure gradient, and are able to create a so called internal transport barrier.

**Introduction**— Being able to sustain a steep density profile in hot magnetized plasma is one of the major key points to achieve magnetically confined fusion devices. These steep profiles are typically associated with the emergence in the plasma of so-called internal transport barriers (ITB) [1, 2]. Both the creation and study of these barriers have generated numerous investigations mostly numerical using either a fluid, or magnetic field or kinetic perspective or combining some of these. In this paper starting from the direct study of particle motion, we propose a simple mechanism to create such barriers which may not have been fully considered yet. Indeed, charged particle motion in a non-uniform magnetic field [3–9] is one of main classical issues of physics of plasmas in space or in fusion reactors. To tackle this problem the guiding center [7] and the gyrokinetic [8] theories are developed to trace the particle’s slower motion by averaging the faster cyclotron motion. These reductions suppress computational cost and they are widely used to simulate the magnetically confined plasmas in fusion reactors [6]. These reduction theories assume existence of an invariant or an adiabatic invariant of motion associated with the magnetic moment  $\mu_0$ . Meanwhile, this assumption does not always hold true. Then, recently, studies on full particle orbits without any reductions are done to look into phenomena ignoring by these reductions and to interpolate the guiding center orbit. There exists a case that a guiding center trajectory and a full trajectory are completely different [10]. Further, it is found that the assumption of the invariant  $\mu_0$  breaks [11, 12] due to the chaotic motion of the test particles.

Let us quickly review the single particle motion and adiabatic chaos. We consider a model of charged particle moving in a non-uniform cylindrical magnetic field  $\mathbf{B}(r) = \nabla \wedge \mathbf{A}_0(r)$ . The vector potential  $\mathbf{A}_0(r)$  is given by

$$\mathbf{A}_0(r) = -\frac{B_0 r}{2} \mathbf{e}_\theta - B_0 F(r) \mathbf{e}_z, \quad F(r) = \int_0^r \frac{r dr}{R_{\text{per}} q(r)}, \quad (1)$$

where the cylinder is parametrized with the coordinate  $(r, \theta, z)$ ,  $B_0$  is strength of the magnetic field,  $z$  has  $2\pi R_{\text{per}}$  periodicity,  $\mathbf{e}_\theta$  and  $\mathbf{e}_z$  are basic units for each direction, and  $q(r)$  is a winding number called a safety factor of magnetic

field lines. The Hamiltonian of the particle  $H = \|\mathbf{v}\|^2/2$ , where  $\mathbf{v}$  denotes particle’s velocity, has three constants of motion, the energy, the angular momentum, and the momentum, associated with time, rotational, and translational symmetry of the system respectively, so that the Hamiltonian  $H$  on the six dimensional phase space is reduced into the single-degree-of-freedom Hamiltonian on the two dimensional phase space,  $(r, p_r)$ -plane [11, 12],

$$H_{\text{eff}}(r, p_r) = p_r^2/2 + V_{\text{eff}}(r),$$

$$V_{\text{eff}}(r) = \frac{v_\theta^2 + v_z^2}{2} = \frac{(p_\theta^2 r^{-1} - B_0 r/2)^2}{2} + \frac{(p_z + B_0 F(r))^2}{2}. \quad (2)$$

where  $p_i$  stands for the conjugate momentum for  $i = r, z$ , and  $\theta$  respectively, and where  $v_\theta = r\dot{\theta}$  and  $v_z = \dot{z}$ . The upper dot denotes  $d/dt$ . Invariants  $p_z$  and  $p_\theta$  are fixed by an initial condition. Appropriately setting the safety factor  $q$  and choosing initial condition, we can find an unstable fixed point in  $(r, p_r)$  phase plane, which can induce the adiabatic chaos [13–17] when the weak magnetic perturbation or the curvature effect added to the flat torus (cylinder) exist [11, 12].

This Letter aims to exhibit one possibility that the unstable fixed point inducing chaotic motion modifies mesoscopic properties of plasmas, a local density and a local pressure gradient which is believed to be associated with the internal transport barriers (ITBs) [1, 2] a feature that may be missed by gyrokinetics, or a pure magneto-hydrodynamic approach.

For this purpose, this Letter deals with the radial density function  $\rho(r)$  derived from the maximal entropy principle, which is a steady state of a truncated Vlasov-Maxwell system with an ion moving in a static magnetic field and null electric field and without an effect of electrons, radiation from moving particles, and back reaction from fields. We qualitatively discuss which kind of vector potentials  $F(r)$  or  $q$ -profiles are likely to bring about the unstable fixed point for the test particle motion. Then, we look into the effect of the unstable fixed point for the density profile and the local-pressure gradient. We shall end this Letter by remarking the relation between particle’s ITBs and the magnetic

ITBs [18, 19].

*Equilibrium radial density function*— The Vlasov-Maxwell system consists of the collisionless Boltzmann equation describing a temporal evolution of single particle density functions of ions and electrons, coupled with the Maxwell equation determining a self-consistent electro-magnetic field [20, 21]. Before dealing with such a very complex system, it is worthwhile to consider the test particle motion in static nonuniform magnetic fields. We neglect electrons, inter-particle interactions, radiation from moving charged particles and back reaction from the electro-magnetic field. The Boltzmann's constant  $k_B$  is set as unity. Let us consider a steady state associated with a density function  $f_0$  on the phase space, which commutes with Hamiltonian (2) and maximizes the information entropy

$$\mathcal{S}[f] = - \iint_{\mu} f \ln f d^3 \mathbf{p} d^3 \mathbf{q}, \quad (3)$$

subject to the normalization condition and energy, momentum, and angular momentum conservations, which are respectively

$$\begin{aligned} \mathcal{N}[f] &= \iint_{\mu} f d^3 \mathbf{p} d^3 \mathbf{q}, & \mathcal{E}[f] &= \iint_{\mu} H_{\text{eff}} f d^3 \mathbf{p} d^3 \mathbf{q}, \\ \mathcal{P}[f] &= \iint_{\mu} p_z f d^3 \mathbf{p} d^3 \mathbf{q}, & \mathcal{L}[f] &= \iint_{\mu} p_{\theta} f d^3 \mathbf{p} d^3 \mathbf{q}, \end{aligned} \quad (4)$$

where the integral  $\iint_{\mu} \bullet d^3 \mathbf{p} d^3 \mathbf{q}$  means average over the six dimensional single particle phase space, called  $\mu$ -space [22]. The solution to this variational problem is

$$f_0 = e^{-\beta H_{\text{eff}} - \gamma_1 - \gamma_{\theta} p_{\theta} - \gamma_z p_z} \quad (5)$$

where  $\beta$ ,  $\gamma_1$ ,  $\gamma_{\theta}$ , and  $\gamma_z$  are the Lagrangian multipliers, associated with energy conservation, normalization, momentum and angular momentum conditions respectively. The parameter  $\beta$  corresponds to the thermodynamical temperature as  $T_{\text{th}}^{-1} \equiv \beta = \delta \mathcal{S} / \delta \mathcal{E}$ , so that it must be positive. It should be noted that  $-\gamma_{\theta}$  and  $-\gamma_z$  are proportional to the ensemble averages of  $v_{\theta}$  and  $v_z$  respectively. When the ITB exists, it is believed that the plasmas rotation exists, so that the averages of  $v_{\theta}$  and  $v_z$  are not 0 and so are  $\gamma_{\theta}$  and  $\gamma_z$ , which are negative. The spatial density function  $n(\mathbf{q})$  is deduced from this result as

$$n(\mathbf{q}) \equiv \int f_0 d^3 \mathbf{p} = \int f_0 r^{-1} d p_{\theta} d p_z d p_r. \quad (6)$$

Thus, the density  $n(r) d^3 \mathbf{q}$  is proportional to

$$n(\mathbf{q}) r dr d\theta dz \propto e^{\left(\frac{\gamma_{\theta}}{2} \left(-B_0 - \frac{\gamma_{\theta}}{\beta}\right) r^2 + \gamma_z B_0 F(r)\right)} r dr d\theta dz, \quad (7)$$

and is independent of  $\theta$  and  $z$ . We then obtain a radial density function  $\rho(r)$  given by

$$\rho(r) = \frac{\iint n(\mathbf{q}) r dr d\theta dz}{\iint r dr d\theta dz} = \frac{1}{4\pi^2 r R_{\text{per}}} \iint n(\mathbf{q}) r dr d\theta dz, \quad (8)$$

as

$$\begin{aligned} \rho(r) &= \frac{\exp(-ar^2 - bF(r))}{\int_0^1 \exp(-ar^2 - bF(r)) dr}, \\ a &= -\frac{\gamma_{\theta}}{2} \left(-B_0 - \frac{\gamma_{\theta}}{\beta}\right), \quad b = -\gamma_z B_0. \end{aligned} \quad (9)$$

It should be noted that the local pressure  $P(r)$  is proportional to the radial density  $\rho(r)$ , because we assume the equation of state  $P(r) = \rho(r) T_{\text{th}}$  holds locally true.

*Unstable fixed point of test-ion-particle*— We now move on and consider how the existence of the unstable fixed points with relevant energy level affect to the obtained equilibrium density profile. For this purpose we have to discuss how the safety factor is chosen, in other words which function  $F$  in Eq. (1) leads to the emergence of “practical” unstable points in the effective potential  $V_{\text{eff}}$ . Indeed, as a first point to pin out, if the amplitude of  $F$  is large, we can expect that the term  $v_z^2/2 = (p_z + F)^2/2$  in the Hamiltonian (2) becomes also large, then the unstable points appear in the phase space at so high energy level that they become physically irrelevant. Then, the amplitude of  $F$  should be small.

Moreover if the variations of  $F(r)$  are smooth and “gentle” with  $r$ , so does again  $(p_z + F)^2/2$  in  $V_{\text{eff}}$ , then  $V_{\text{eff}}$  has only one minimum point that is essentially governed by the term  $(p_{\theta}/r - B_0/2)^2/2$ . Thus, the enough concavity of  $v_z^2/2$  near but not at the minimum point of  $(p_{\theta}/r - B_0/2)^2/2$ ,  $r = \sqrt{2p_{\theta}/B_0}$  is necessary for that  $V_{\text{eff}}$  has unstable points. These considerations are illustrated in Fig. 1. In the panel (d), we assume that there exists an  $r$  such that  $p_z + F(r) = 0$ . We stress out as well that if  $|p_z|$  is sufficiently large, it is also possible to create an unstable point, but then again the energy level is so high that it is irrelevant for the mesoscopic profiles in plasmas.

It has been known for a while that the presence of chaos affects sometimes averages the density profile locally. For instance, the averaging effect in plasmas from the global chaos induced by the resonance overlapping [23] has been found and it modify the density profile [24]. Even though this in this letter we are directly tackling the passive particle motions of ions and thus a different type of localized chaos, similar things can be expected. In the present case the unstable fixed points are located around the place in which the steepness of density (9) and the local pressure gradient exist. Then, the staircase like density profile as illustrated in Fig. 2 may appear.

Since the safety factor  $q(r)$  can be directly associated with the function  $F(r)$  at the origin of the unstable fixed points, and  $q(r)$  is a crucial parameter for the operation of magnetized fusion machine, let us discuss more how the con-

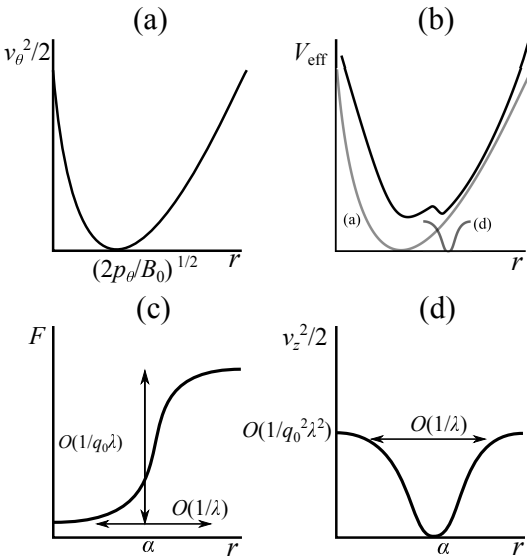


FIG. 1. Schematic picture showing how the saddle point appears around the bottom of safety factors. A Panel (a) represents a part of  $v_\theta^2/2 = (p_\theta/r - B_0 r/2)^2/2$ , (b)  $V_{\text{eff}}$ , (c)  $F(r)$ , and (d)  $v_z^2/2 = (p_z + F(r))^2/2$ . In the panel (d), we consider that there exists an  $r$  such that  $p_z + F(r) = 0$ . The parameters  $q_0$ ,  $\lambda$ , and  $\alpha$  are associated with Eq. (10).

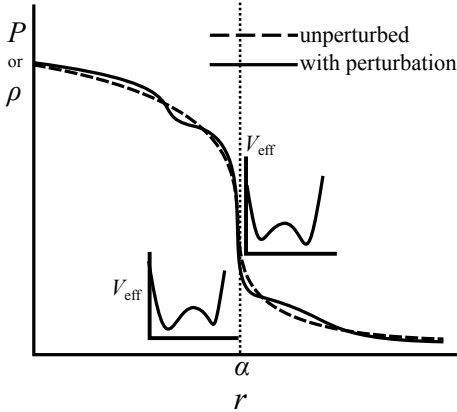


FIG. 2. Schematic picture of the density  $\rho$  or pressure  $P$  profiles. The dashed curve represents unperturbed one and the solid curves one modified with the adiabatic chaos.

straints discussed previously translate on the  $q$ -profile. For instance let us consider a situation with a non-monotonous profile such that  $q(r)$  has a minimum  $q_0$  at  $r = \alpha$  and the spatial scale is characterized with  $\lambda$ . Then locally  $q(r)$  can be expressed as

$$q(r) = q_0 [1 + \lambda^2(r - \alpha)^2], \quad r \sim \alpha. \quad (10)$$

Recalling Eq. (1), the function  $F$  is scaled as  $q_0^{-1}\lambda^{-1}$ , and  $v_z^2/2 = (p_z + F)^2/2 \sim q_0^{-2}\lambda^{-2}$ , so that this is a typical energy level of the particles located near a separatrix. It should be noted that the width of the well of  $v_z^2/2$  is scaled as  $\lambda^{-1}$  (see Fig. 1). For a fixed value of  $q_0$ , a large value of  $\lambda$  creates un-

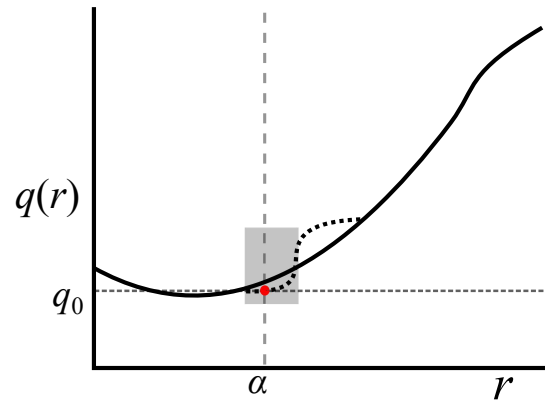


FIG. 3. Schematic picture exhibiting how to create unstable fixed point by modifying  $q$ -profile. The solid curve represents the given  $q$ -profile. The broken curve represents the modified  $q$ -profile which is fitted by  $q_0(1 + \lambda^2(r - \alpha)^2)$  in a shaded region.

stable fixed points with relevant energy level for the particle whose angular momentum  $p_\theta \sim B_0 \alpha^2/2$ . As  $\lambda$  gets to be larger, the number of the particles with unstable fixed point increase, this is because, roughly speaking, the energy level of unstable points gets to be lower, and the one-particle density (5) is proportional to  $e^{-\beta H_{\text{eff}}}$ .

As a consequence of these consideration we illustrate on Fig. 3 how to adjust a given  $q$ -profile to create unstable fixed point whose location is  $r \sim \alpha$ . This is similar to what is done in Ref. [19], to create flat region of  $q$ -profile to create an ITB with a magnetic field line perspective.

*Example*— The previous discussions can be considered quite qualitative, in order to be more explicit we consider a specific example, for which we shall exhibit that the emergence of unstable fixed points induce the presence of a local ITB in their vicinity, i.e their radial positions are inducing the existence locally strong density gradients. For this purpose we simply consider the  $q$ -profile given by Eq. (10) with parameters  $q_0 = 0.12$ ,  $\lambda = 55$ , and  $\alpha = \sqrt{0.18} \simeq 0.4243$ , in Figs. 4 and 5. The adiabatic chaos due to separatrix crossing in this magnetic field has been discussed in Ref. [11]. The results are displayed in Fig. 4, where various density profiles (9) obtained for several parameters  $a$  and  $b$  are shown. We find the steep region which corresponds to the local steep density gradient and the ITBs appear around  $r = \alpha$  on which  $q(r)$  satisfies  $q'(r) = 0$ . In Fig. 5, we exhibit the locations of unstable fixed points and their energy levels. We can notice that the unstable fixed points appear in  $r \simeq \alpha$  but not on exactly on  $r = \alpha$ . Regarding the relation between the precise location of the fixed points and the barrier position and height a more precise systematic study will be performed in future work for a longer paper.

*Internal transport barrier*— Before concluding this letter we would like to make some remarks on the observed ITBs. We would like to stress out the similarities and differences between our observations and the magnetic ITBs discussed for instance in [19]. One of the main difference is

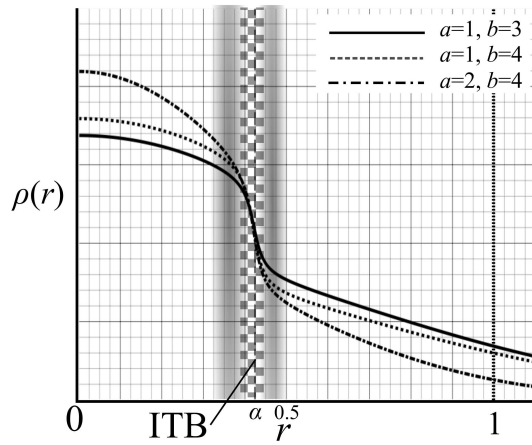


FIG. 4. Density profile for the unperturbed system and the chaotic region (gray-painted) for the perturbed system. Checker board region represents an ITB. The parameters in a local  $q$ -profile [Eq. (10)] are determined as  $q_0 = 0.12$ ,  $\lambda = 55$ ,  $\alpha = \sqrt{0.18} \approx 0.4243$ .

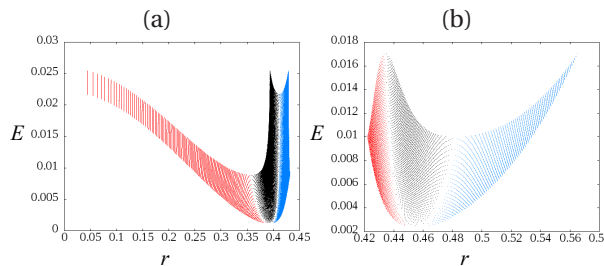


FIG. 5. (Color online) Black dotted region (center) represents a set of saddle points. The parameters in a local  $q$ -profile [Eq. (10)] are determined as  $q_0 = 0.12$ ,  $\lambda = 55$ ,  $\alpha = \sqrt{0.18} \approx 0.4243$ . The blue (right) and red (left) regions represent elliptic points respectively. The energy  $E$  is given by the energy at saddle point for each effective Hamiltonian. The panel (a) and (b) are for the saddle points in the inside and outside of the magnetic ITB respectively.

that if the plateau of  $q(r)$  appears as illustrated in Fig. 3 the transport barrier appears even if the value of  $q$  is far from rational number  $m/n$  with small integers  $m$  and  $n$ , meaning the existence of this barrier does not appear to be correlated to the existence of a resonant surface, on the other hand in the considered example, the location of the magnetic ITB coincides with the place on which the local density gradient exists.

Another study between the particle's motion and the existence of an ITB using a pure field line approach and the existence of a stable magnetic tori has been performed from the view point of the difference between the magnetic winding number  $q(r)$  and the effective one  $q_{\text{eff}}(r)$  for the guiding venter orbit of the energetic particles [25]. In a recent study [26], it is shown that the resonance shift due to the grad  $B$  drift and its disappearance due to the curvature drift effect can create an invariant tori in the particle dynamics while there are none for magnetic field lines, and this is confirmed both analytically and numerically with the full par-

ticile orbits around the resonance points. It should be remarked that the guiding center theory is useless to clarify it unlike Ref. [26].

The above consideration suggests that the other possible difference between the magnetic and the particle's ITBs induced by the separatrices, this is because the two unstable fixed points appear around the magnetic ITB. When the parameter  $\lambda$  in Eq. (10) gets to be large, the steep region of  $\rho(r)$  gets to be small and the influence of the separatrix grows because the gap of  $F(r)$  between  $r < \alpha$  and  $r > \alpha$  becomes smaller (see Fig. 1), as a result we obtain a local steepness of the density and the local pressure gradient around the magnetic ITB. To conclude, we have shown in this letter that internal transport barrier can emerge due to the presence of a separatrix in the passive particle orbits, this phenomenon is not related to the existence of a local resonant surface. We also discussed how the  $q$ -profile can be tuned in order to generate such barriers. Finally we also would like to stress out that the emergence of a separatrix and associated transport barrier can as well occur in monotonous  $q$ -profile, the effect appeared as enhanced when the degeneracy allows two nearby unstable points to appear, a more detail study is left for a longer paper. In future work we will be considering as well the electrons distributions and using these to built self-consistent stationary solutions of the Vlasov equation, in this setting we shall be able to see if self-consistent  $q$ -profile giving rise to transport barrier can emerge as an equilibrium solution or belongs definitely to the out-of equilibrium realm.

*Acknowledgement*— This work has been carried out within the framework of the French Research Federation for Magnetic Fusion Studies. We acknowledge the financial support of the A\*MIDEX project (n°ANR-11-IDEX-0001-02) funded by the “investissements d'Avenir” French Government program, managed by the French National Research Agency (ANR).

\* shun.ogawa@cpt.univ-mrs.fr

† xavier.leoncini@cpt.univ-mrs.fr

‡ valex@iki.rssi.ru

§ xavier.garbet@cea.fr

---

- [1] R. C. Wolf, Internal transport barriers in tokamak plasmas, *Plasma Phys. Control. Fusion* **45**, R1 (2003).
- [2] J. W. Connor, T. Fukuda, X. Garbet, C. Gormezano, V. Mukhovatov, M. Wakatani, ITB Database Group, and ITPA Topical Group on Transport and Internal Barrier Physics, A review of internal transport barrier physics for steady-state operation of tokamaks, *Nucl. Fusion* **44**, R1 (2004).
- [3] H. Alfvén, On the motion of a charged particle in a magnetic field, *Ark. Mat. Astron. Fys.* **27A**, 1 (1940); *Cosmological electrodynamics*, (Oxford university press, London, 1950).
- [4] T. G. Northrop, The guiding center approximation to charged particle motion, *Ann. Phys.* **15**, 79 (1961).
- [5] R. G. Littlejohn, Hamiltonian formulation of guiding center motion, *Phys. Fluids* **24**, 1730 (1981).

- [6] A. H. Boozer, Physics of magnetically confined plasmas, *Rev. Mod. Phys.* **76**, 1071 (2004).
- [7] J. R. Cary and A. J. Brizard, Hamiltonian theory of guiding-center motion, *Rev. Mod. Phys.* **81**, 693 (2009).
- [8] A. J. Brizard and T. S. Hahm, Foundations of nonlinear gyrokinetic theory, *Rev. Mod. Phys.*, **79**, 421 (2007).
- [9] J. D. Jackson, *Classical Electrodynamics*, 3rd ed. (Wiley, USA, 1998).
- [10] D. Pfefferl  , J. P. Graves, and W. A. Cooper, Hybrid guiding-centre/full-orbit simulations in non-axisymmetric magnetic geometry exploiting general criterion for guiding-centre accuracy, *Plasma Phys. Controlled Fusion* **57**, 054017 (2015).
- [11] S. Ogawa, B. Cambon, X. Leoncini, M. Vittot, D. del-Castillo-Negrete, G. Dif-Pradalier, and X. Garbet, Full particle orbit effects in regular and stochastic magnetic fields, *Phys. Plasmas* **23**, 072506 (2016).
- [12] B. Cambon, X. Leoncini, M. Vittot, R. Dumont, and X. Garbet, Chaotic motion of charged particles in toroidal magnetic configurations, *Chaos* **24**, 033101 (2014).
- [13] A. I. Neishtadt, Change of an adiabatic invariant at a separatrix, *Sov. J. Plasma Phys.* **12**, 568 (1986).
- [14] A. I. Neishtadt, On the change in the adiabatic invariant on crossing a separatrix in systems with two degrees of freedom, *Prikl. Matem. Mekhan. USSR* **51**, 586 (1987).
- [15] J. L. Tennyson, J. R. Cary, and D. F. Escande, Change of the adiabatic invariant due to separatrix crossing, *Phys. Rev. Lett.* **56**, 2117 (1986).
- [16] J. R. Cary, D. F. Escande, and J. L. Tennyson, Adiabatic-invariant change due to separatrix crossing *Phys. Rev. A* **34**, 4256 (1986).
- [17] X. Leoncini, A. Neishtadt, and A. Vasiliev, Directed transport in a spatially periodic harmonic potential under periodic nonbiased forcing, *Phys. Rev. E* **79**, 026213 (2009).
- [18] R. Balescu, Hamiltonian nontwist map for magnetic field lines with locally reversed shear in toroidal geometry, *Phys. Rev. E* **58**, 3781 (1998).
- [19] D. Constantinescu and M.-C. Firpo, Modifying locally the safety profile to improve the confinement of magnetic field lines in tokamak plasmas *Nucl. Fusion* **52**, 054006 (2012).
- [20] A. A. Vlasov, The vibrational properties of an electron gas, *Zh. Eksp. Ther. Fiz.* **8**, 291 (1938); *Sov. Phys. Uspekhi* **93** (1968).
- [21] L. P. Pitaevskii and E.M. Lifshitz, *Physical Kinetics* (Butterworth-Heinemann, Oxford, 1981)
- [22] D. Zubarev, V. Morozov, and G. R  pke, *Statistical Mechanics of Nonequilibrium Processes, Volume 1: Basic concepts, kinetic theory* (Academic Verlag, Berlin, 1996).
- [23] B. V. Chirikov, A universal instability of many-dimensional oscillator systems, *Phys. Rep.* **52**, 263 (1979).
- [24] R.B. White, Modification of particle distributions by MHD instabilities I, *Commun. Nonlinear Sci. Numer. Simulat.* **17**, 2200 (2012); Modification of particle distributions by MHD instabilities II, *Plasma Phys. Control. Fusion* **53**, 085018 (2011).
- [25] G. Fiksel, B. Hudson, D. J. Den Hartog, R. M. Magee, R. O'Connell, and S. C. Prager, Observation of weak impact of a stochastic magnetic field on fast-ion confinement, *Phys. Rev. Lett.* **95**, 125001 (2005).
- [26] S. Ogawa, X. Leoncini, G. Dif-Pradalier, and X. Garbet, Study on creation and destruction of transport barriers via effective safety factors for energetic particles, arXiv:1610.02867.